CHEMICAL ENGINEERING TRANSACTIONS
VOL. 71, 2018
A publication of AIDIC
The Italian Association of Chemical Engineering
Online at www.aidic.it/cet
Guest Editors: Xiantang Zhang, Songrong Qian, Jianmin Xu

**ISBN** 978-88-95608-68-6; **ISSN** 2283-9216
DOI: 10.3303/CET1871168

# MHD Flow Analysis with Water-based CNT Nanofluid over a Non-linear Inclined Stretching/Shrinking Sheet Considering Heat Generation

S.R.R. Reddy[a], P. Bala Anki Reddy[a,*], Ali J. Chamkha[b,c]

[a] Department of Mathematics, SAS, Vellore Institute of Technology, Vellore-632014, India.
[b] Mechanical Engineering Department, Prince Sultan Endowment for Energy and Environment, Prince Mohammad Bin Fahd University, Al- Khobar 31952, Saudi Arabia.
[c] RAK Research and Innovation Center, American University of Ras Al Khaimah, P.O. Box 10021, Ras Al Khaimah, United Arab Emirates.
pbarmaths@gmail.com

This paper presents a numerical analysis of the magnetohydrodynamic (MHD) flow of Carbon nanotube (CNT) nanofluid over a non-linear inclined stretching/shrinking sheet with heat generation and viscous dissipation. In this model, we used SWCNT-$H_2O$ and MWCNT- $H_2O$ as Nano liquids. By using the self-similar numerical solutions, the governing non-linear momentum and thermal boundary layer equations rehabilitated to ordinary differential equations. The resultant mathematical model is numerically solved with the assistance of R-K fourth order with shooting technique. Numerical exploration is completed by inspecting the various values of a magnetic field parameter, non-linear stretching/shrinking parameter, Richardson number, Eckert number, effective Prandtl number and a suction parameter for the flow and heat transfer which are obtainable through graphs. It is found that SWCNT-$H_2O$ nano liquid produce high heat transfer compared to MWCNT- $H_2O$ nano liquid. The validity of calculated results is analysed through the qualified level.

## 1. Introduction

In Physics, the Nano-materials are very new, attractive and the carbon nanotubes are a high aspect ratio of carbon-based nanomaterial. Carbon nanotubes can be classified into two types, they are SWCNT's and MWCNT's. Both the CNTs have high thermal conductivity and electrical conductivity comparatively. This paper focuses on nanofluids containing the nanoparticles. The known nanofluid was initiated by (Choi et al., 1995), he submerged the nanofluid particles of SWCNT's and MWCNT's in water. The latest results show that nanofluid executes higher thermal conductivity than that of the base fluid, which are water, lubricants, oil and ethylene glycol. Various nanoparticles which incorporate CNTs, copper, silver, and titanium aluminium metals with/without their oxides are of awesome logical enthusiasm as they connect mass materials and atomic structures. The thermal conductivity of the nanoparticles is high when contrasted with the conventional base liquids like ethylene glycol, oil, water and so on, as confirmed in test contemplates focused by (Eastman et al., 2001; Xuan et al., 2003). In nanofluid, the stretching/shrinking sheet has transported a significant interest for researchers owed to its gigantic applications in business and engineering fields. With preceding references, there are two main ways in the shrinking sheet case, when the flow towards a shrinking sheet exists, it is to execute the first acceptable mass suction on the boundary (Miklavcic et al., 2006), whereas remaining is for stagnation point flow (Wang 2008). Numerical examination of heat exchange and thick stream over a non-linearly extending sheet has been directed for a Newtonian liquid was examined by (Cortell 2007) with different thermal boundary conditions utilizing a Runge-Kutta (RK) calculation.
Two-dimensional stagnation point flow of CNT +$H_2O$ towards an extending sheet affected by slip effect and convective limit condition was examined by (Akbar et al., 2014). He is observed that because of high thickness and thermal conductivity of SWCNT, the Nusselt number for SWCNT is higher when compared with the MWCNT. In his examination, thermal conductivity and thickness of both SWCNT and MWCNT inside the base

Please cite this article as: Reddy S., Reddy P.B.A., Chamkha A.J., 2018, Mhd flow analysis with water-based cnt nanofluid over a non-linear inclined stretching/shrinking sheet considering heat generation, Chemical Engineering Transactions, 71, 1003-1008
DOI:10.3303/CET1871168

liquids (water, ethylene glycol and engine oil) of the comparable volume were researched by (Haq et al., 2015) when the liquid was streaming over an extending surface. The carbon particles premise starts interesting updraft property with massive updraft conductivities because of the tubular type of carbon particles premise. These are recorded as Carbon nanotubes (CNTs). The span of CNTs accumulation from 1 nm to 100 nm and have lengths in micrometre. The single and multi-wall carbon nanotubes having their thermal conductivity, 6600 W/m-K and 3000 W/m-K respectively and further thermal conductivity model details are presented in Refs. (Pal et al., 2013; Hong et al., 2007; Kumar et al., 2018; Akbara et al., 2018; Reddy et al., 2012; Hussain et al., 2018; Rashid et al., 2017).
Motivated from the above examination, the aim of the present study is to analyzing the magnetohydrodynamic (MHD) flow of Carbon nanotube (CNT) nanofluid over a non-linear inclined stretching/shrinking sheet with heat generation and viscous dissipationthe.

## 2. Mathematical formulation

We consider laminar, 2D, steady, incompressible magnetohydrodynamic (MHD) flow of Carbon nanotube (CNT) nanofluid over a non-linear inclined stretching/shrinking sheet. Let $\alpha$ as the vertical inclined angle and its considered SWCNT and MWCNT type of CNT's. The sheet is extended with a velocity $u_w(x) = cx^n$, where *n, c* are the nonlinear stretching parameter and constant. We have taken *x*-axis along the stretching/shrinking sheet directly, *y*-axis is normal to it. The flow is expected at $y \geq 0$ and takes the value of temperature is constant $T_w > 0$ at stretching/shrinking sheet although by the temperature of ambient nanofluid $T_\infty$ takes the constant value as $y \to \infty$. A constant magnetic field $B(x) = B_0 x^{0.5(m-1)}$ is executed in a transverse way. Here the base fluid and submerged nanoparticles are in thermal equilibrium. Under these assumptions, the principal equations that are based on the conservation of mass, momentum and energy can be expressed in the following form:

$$\frac{\partial u}{\partial x} + \frac{\partial u}{\partial y} = 0 \tag{1}$$

$$u\frac{\partial u}{\partial x} + v\frac{\partial u}{\partial y} = \frac{\mu_{nf}}{\rho_{nf}}\frac{\partial^2 u}{\partial y^2} + g\beta(T - T_\infty)\cos(\alpha) - \frac{\sigma B^2(x)}{\rho_{nf}}\sin^2\xi u \tag{2}$$

$$u\frac{\partial T}{\partial x} + v\frac{\partial T}{\partial y} = \alpha_{nf}\frac{\partial^2 T}{\partial y^2} - \frac{1}{(\rho c_p)_{nf}}\frac{16\sigma^* T_\infty^3}{3k^*}\frac{\partial^2 T}{\partial y^2} + \frac{\mu_{nf}}{(\rho c_p)_{nf}}\left(\frac{\partial u}{\partial y}\right)^2 + \frac{\sigma B^2(x)}{(\rho c_p)_{nf}}\sin^2\xi u^2 + \frac{Q_0}{(\rho c_p)_{nf}}(T - T_\infty) \tag{3}$$

Subject to the boundary conditions:

$$\begin{aligned} &u_w(x) = \pm Cx^m,\ v = v_w,\ T = T_w(\mathrm{x}) = \mathrm{T}_\infty + bx^n \text{ at } y = 0 \\ &u \to 0,\ T \to T\infty \text{ as } y \to \infty \end{aligned} \tag{4}$$

Here c is constant i.e., $c > 0$ and $c < 0$ are the stretching sheet and shrinking sheet respectively, $\rho_{nf}$ is the effective density for the nanofluid, $\sigma$ is the thermal diffusivity of the nanofluid, $\mu_{nf}$ is the dynamic viscosity coefficient of the nanofluid, $(\rho c_p)_{nf}$ is the heat capacity coefficient regarding nanofluid are defined as below:

$$\left.\begin{aligned} &\alpha_{nf} = \frac{k_{nf}}{(\rho c_p)_{nf}}, \mu_{nf} = \frac{\mu_f}{(1-\varphi)^{2.5}}, \rho_{nf} = \varphi\rho_{CNT} + \rho_f(1-\varphi), (\rho c_p)_{nf} = \varphi(\rho c_p)_{CNT} + (\rho c_p)_f(1-\varphi), \\ &\frac{k_{nf}}{k_f} = \frac{(1-\phi) + 2\phi\frac{k_{CNT}}{k_{CNT}-k_f}\ln\frac{k_{CNT}+k_f}{2k_f}}{(1-\phi) + 2\phi\frac{k_f}{k_{CNT}-k_f}\ln\frac{k_{CNT}+k_f}{2k_f}}, \end{aligned}\right\} \tag{5}$$

### 2.1 Method of solution

Now we defining new similarity variables

$$\psi=\left[\frac{2\nu_f x u_w(x)}{(m+1)}\right]^{1/2} f(\eta),\eta=\left[\frac{(m+1)u_w(x)}{2\nu_f x}\right]^{1/2} y,\theta(\eta)=\frac{T-T_\infty}{T_w-T_\infty} \tag{6}$$

Where $\psi$ is the stream function and $\nu_f$ is the kinematic viscosity of a fluid then here we define stream function as: $u=\frac{\partial\psi}{\partial y},v=-\frac{\partial\psi}{\partial x}$. By using the above variables leads to getting the below nonlinear differential equations.

$$\frac{1}{(1-\phi)^{2.5}}f'''+\left((1-\phi)+\phi\frac{\rho_{CNT}}{\rho_f}\right)\left(ff''-\frac{2m}{m+1}f'^2\right)+\frac{2}{m+1}\left((1-\phi)+\phi\frac{(\rho)_{CNT}}{(\rho)_f}\right)(Ri\cos(\alpha))\theta-M\sin^2(\xi)f'=0 \tag{7}$$

$$\frac{1}{\mathrm{Pr}_{eff}}\theta''+\left((1-\phi)+\phi\frac{(\rho c_p)_{CNT}}{(\rho c_p)_f}\right)\left(f\theta'-\left(\frac{2n}{m+1}\right)f'\theta\right)+\frac{Ec}{(1-\phi)^{2.5}}(f'')^2+\frac{1}{m+1}\frac{Q}{\mathrm{Pr}}\theta+\frac{1}{\mathrm{Pr}}EcM^2\sin^2\xi\, f'^2=0 \tag{8}$$

The boundary conditions:

$$f(0)=S,\ f'(0)=\pm1,\ \theta(0)=1,\ f'(\infty)\to0,\ \theta(\infty)\to0 \tag{9}$$

Where *M* is a magnetic parameter, *Ri* is the Richardson number, *Gr* is the Grashof number, $\mathrm{Re}_x$ is the local Reynolds number, $\mathrm{Pr}_{eff}$ is effective Prandtl number, *Q* is the heat source/sink parameter, *Ec* is the Eckert number, *Nr* is the thermal radiation parameter and *S* is the suction parameter. The above all parameters we defined as

$$M=\frac{2\sigma B_0^2}{c(m+1)\rho_f},Gr=\frac{g\beta(T_w-T\infty)x^3}{\nu_f^2},Nr=\frac{-16\sigma^*T_\infty^3}{3k_f k^*},\mathrm{Re}_x=\frac{xu_w(x)}{\nu_f},Ec=\frac{u_w^2}{(c_p)_f(T_w-T_\infty)},$$

$$Q=\frac{Q_0 2\nu_f k}{k_f u_w(x)},Ri=\frac{Gr}{\mathrm{Re}_x^2},\mathrm{Pr}_{eff}=\mathrm{Pr}/\left(\frac{k_{nf}}{k_f}+Nr\right),S=\frac{-2v_w x^{-(m-1)/2}}{(m+1)\sqrt{c\nu_f}}. \tag{10}$$

The coefficient of skin friction $C_f$ and Nusselt number $Nu_x$ are the physical quantities which are defined as

$$C_f=\frac{\mu_{nf}}{\rho_f u_w^2}\left(\frac{\partial u}{\partial y}\right)_{y=0},Nu_x=\frac{-xk_{nf}}{k_f(T_w-T_\infty)}\left(-\frac{\partial T}{\partial y}\right)_{y=0} \tag{11}$$

We described the non-dimensional form from the above equations (Eq.10 and 15)

$$\mathrm{Re}_x^{1/2}C_f=\frac{1}{(1-\varphi)^{2.5}}\left(\frac{m+1}{2}\right)^{1/2}f''(0),\mathrm{Re}_x^{-1/2}Nu_x=-\frac{k_{nf}}{k_f}\left(\frac{m+1}{2}\right)^{1/2}\theta'(0) \tag{12}$$

## 3. Results and discussion

Keeping in mind the end goal to confirm the precision of the present numerical strategy, we have contrasted our outcomes for *f''*(0) with those of Cortell (2007) and Dual Pal et al., (2013) for various estimations of *m* which are exhibited in Tables 1. It is seen from these tables that, the present outcomes coincide very well with their outcomes which endorse that the numerical technique utilized in this paper is perfect and precise. The calculated values of *f''*(0) and -$\theta'$(0) are presented in Tables 2 and 3 for various estimations of *M*, $\xi$, *S, Ri, Q, Ec* and *m* for both extending and contracting cases. From Table 2, It is divulged that the skin-friction coefficient increases with an increase in the aligned angle, Richardson number, heat source and Eckert number whereas the reverse trend is observed for the magnetic parameter, mass flux parameter and non-linear stretching parameter for both cases of SWCNT and MWCNT. It is perceived that the Nusselt number decreases with an increase in the magnetic parameter, heat source and Eckert number, whereas the contrary trend is observed for the aligned angle, mass flux parameter, Richardson number and non-linear stretching parameter for the cases of SWCNT and MWCNT. Further, from Table 3, one can note that the skin-friction coefficient increases with an increase in the magnetic parameter, mass flux parameter, Richardson number,

heat source, Eckert number and non-linear stretching parameter, while the contrary pattern is observed for the aligned angle for both cases of SWCNT and MWCNT. In addition, the value of the Nusselt number decreases as the aligned angle, mass flux parameter, heat source, Eckert number and non-linear stretching parameter, whereas the converse effect is observed by increasing the values of the magnetic parameter and Richardson number for both cases of SWCNT and MWCNT.

The effects of innumerable parameters are probed on the velocity and temperature profiles for both extending and contracting cases cases which are portrayed in Figs.1–12. Figs. 1 and 2 demonstrate the sway of a velocity profile for different values of the magnetic parameter. From these figures, it is divulged that the velocity decreases with rising in magnetic field parameter. This is owing to the fact that, an upsurge in magnetic parameter implies an enrichment of Lorentz force, thus falling the magnitude of the velocity. Figs. 3 and 4 illustrates the velocity profile for different values of angle of inclination. Here we witnessed from Fig. 3 that the velocity drops with increasing the values of angle of inclination for the extending case. From Fig.4, we found that increases the velocity profile by increasing angle of inclination for contracting case. The influence of Richardson number on velocity profiles for extending and contracting cases is exemplified in Figs. 5 and 6. From Fig.5, we professed that the velocity profile increases with increasing the Richardson number for extending case. From Fig. 6, we found that decrease the velocity profile for contracting case with increasing Richardson number. The dimensionless velocity for numerous values of aligned angle is illustrated in Figs.7 and 8. From Fig. 7, we observed that decreases the velocity profile for extending case with an increasing value of aligned angle. From Fig. 8, we noticed that velocity profile falls initially and then rises for contracting case with an increasing value of aligned angle. The outcome of the temperature profile for various estimations of Eckert number for both extending and contracting cases is exhibited in Figs. 9 and 10 respectively. It is apparent that thermal boundary layer is enlarged due to increase in Eckert number for both extending and contracting cases. Figs.11 and 12 expose the temperature profile for various estimations of effective Prandtl number for extending and contracting cases respectively. We infer from these figures that temperature decreases with respect to the effective Prandtl number for extending and contracting cases with increasing values of the effective Prandtl number.

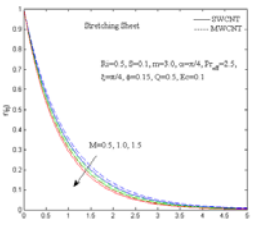


*Figure 1: Effect of M on f'.*

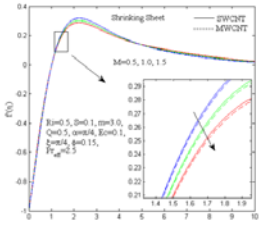


*Figure 2: Effect of M on f.*

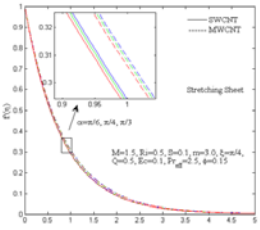


*Figure 3: Effect of $\alpha$ on f'*

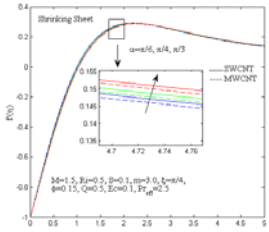


*Figure 4: Effect of $\alpha$ on f'.*

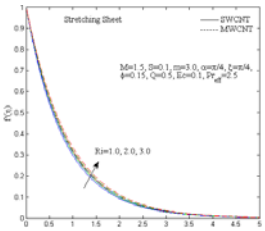


*Figure 5: Effect of Ri on f.*

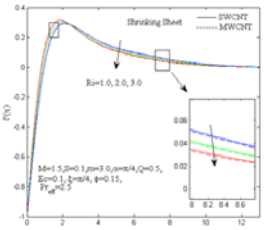


*Figure 6: Effect of Ri on f'*

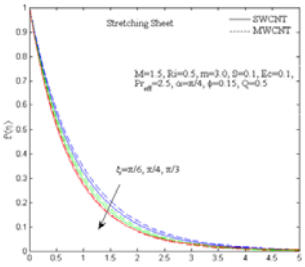


*Figure 7: Effect of $\xi$ on f'.*

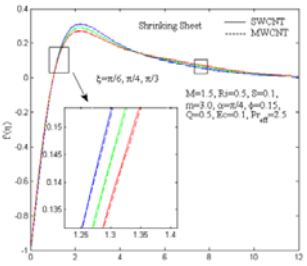


*Figure 8: Effect of $\xi$ on f'.*

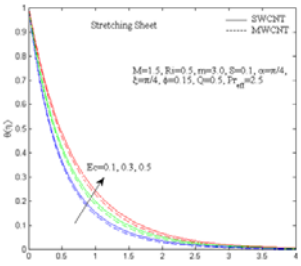


*Figure 9: Effect of Ec on $\theta$*

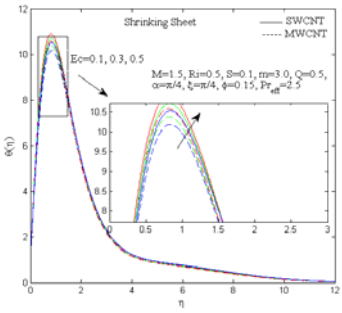


*Figure 10: Effect of Ec on $\theta$*

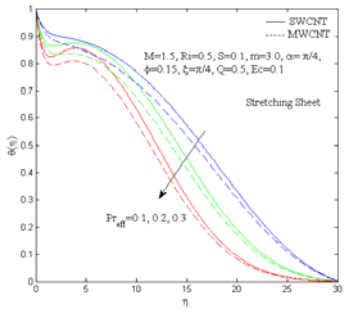


*Figure 11: Effect of $Pr_{eff}$ on $\theta$.*

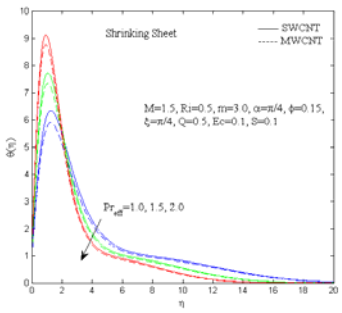


*Figure 12: Effect of $Pr_{eff}$ on $\theta$.*

*Table 1: Comparison of results for -f''(0) for various values of m when $\phi$=M=Ri= 0 for stretching sheet*

| *m* | Cortell (2007) | Dual Pal et al., (2013) | Present results |
|---|---|---|---|
| 0.5 | 0.8895 | 0.8895 | 0.88955 |
| 1.0 | 1.0000 | 1.0000 | 1.00000 |
| 3.0 | 1.1486 | 1.1486 | 1.14860 |
| 10.0 | 1.2349 | 1.2349 | 1.23488 |

*Table 2: Numerical values of skin friction coefficient f''(0) and Nusselt number -$\theta'$(0) for the values of M, S, Ri,Q, Ec, m, $\xi$ for stretching sheet*

| *M* | *ξ* | *S* | *Ri* | *Q* | *Ec* | *m* | SWCNT | | MWCNT | |
|---|---|---|---|---|---|---|---|---|---|---|
| | | | | | | | f''(0) | -θ'(0) | f''(0) | -θ'(0) |
| 1.5 | $\pi/4$ | 0.1 | 0.5 | 0.5 | 0.1 | 3.0 | -1.273281 | 2.181929 | -1.214997 | 2.224807 |
| 0.5 | $\pi/4$ | 0.1 | 0.5 | 0.5 | 0.1 | 3.0 | -1.133050 | 2.272130 | -1.067698 | 2.315976 |
| 1.5 | $\pi/3$ | 0.1 | 0.5 | 0.5 | 0.1 | 3.0 | -1.169670 | 2.239424 | -1.106331 | 2.282593 |
| 1.5 | $\pi/4$ | 0.75 | 0.5 | 0.5 | 0.1 | 3.0 | -1.577559 | 3.004221 | -1.480648 | 3.064943 |
| 1.5 | $\pi/4$ | 0.1 | 1.0 | 0.5 | 0.1 | 3.0 | -1.243434 | 2.195850 | -1.185229 | 2.237648 |
| 1.5 | $\pi/4$ | 0.1 | 0.5 | 1.0 | 0.1 | 3.0 | -1.267264 | 1.820649 | -1.210576 | 1.901280 |
| 1.5 | $\pi/4$ | 0.1 | 0.5 | 0.5 | 0.3 | 3.0 | -1.270044 | 1.854276 | -1.211861 | 1.916391 |
| 1.5 | $\pi/4$ | 0.1 | 0.5 | 0.5 | 0.1 | 2.0 | -1.227145 | 2.123208 | -1.171666 | 2.161521 |

*Table 3: Numerical values of skin friction coefficient f''(0) and Nusselt number -$\theta'$(0) for the values of M, S, Ri,Q, Ec, m, $\xi$ for shrinking sheet*

| *M* | *ξ* | *S* | *Ri* | *Q* | *Ec* | *m* | SWCNT | | MWCNT | |
|---|---|---|---|---|---|---|---|---|---|---|
| | | | | | | | f''(0) | -θ'(0) | f''(0) | -θ'(0) |
| 1.5 | $\pi/4$ | 0.1 | 0.5 | 0.5 | 0.1 | 3.0 | 1.130268 | -22.610880 | 1.165627 | -21.910830 |
| 0.5 | $\pi/4$ | 0.1 | 0.5 | 0.5 | 0.1 | 3.0 | 1.026504 | -23.611170 | 1.062827 | -22.804296 |
| 1.5 | $\pi/3$ | 0.1 | 0.5 | 0.5 | 0.1 | 3.0 | 1.053018 | -23.370121 | 1.089115 | -22.592323 |
| 1.5 | $\pi/4$ | 0.75 | 0.5 | 0.5 | 0.1 | 3.0 | 1.436122 | -27.302318 | 1.438521 | -27.924568 |
| 1.5 | $\pi/4$ | 0.1 | 1.0 | 0.5 | 0.1 | 3.0 | 1.236707 | -12.555924 | 1.271549 | -12.252935 |
| 1.5 | $\pi/4$ | 0.1 | 0.5 | 1.0 | 0.1 | 3.0 | 1.402253 | -31.005721 | 1.429916 | -30.291161 |
| 1.5 | $\pi/4$ | 0.1 | 0.5 | 0.5 | 0.3 | 3.0 | 1.148149 | -23.493463 | 1.183421 | -22.818216 |
| 1.5 | $\pi/4$ | 0.1 | 0.5 | 0.5 | 0.1 | 2.0 | 1.087506 | -14.234012 | 1.122552 | -13.797710 |

## 4. Conclusions

Finally, we stated in our study to acquire the nonlinearly stretching sheet and shrinking sheet flow of nanofluid. In energy equation immersion of radiative heat flux is designated through the Roseland approximation. The ensuing concluding remarks acquired by graphical depiction are:

As the estimations of magnetic field parameter increases, the velocity profiles for extending and contracting cases decreases.
With expanding estimations of aligned angle, the velocity profile is diminished at first and then enlarged for shrinking case.
With increasing values of effective Prandtl number, the temperature profile is increased initially and then decreased for shrinking case.
As the estimations of non-linear stretching parameter rise, skin friction coefficient decreases for both shrinking case and stretching case.

**References**

Akbar N.S., Khan Z.H., Nadeem S., 2014, The combined effects of slip and convective boundary conditions on stagnation-point flow of CNT suspended nanofluid over a stretching sheet, J Mol Liq, 196, 21–25. DOI: 10.1016/j.molliq.2014.03.006

Akbar N.S., Tripathi D., Khan Z.H., 2018, Numerical investigation of cattanneo-christov heat flux in CNT suspended nanofluid flow over a stretching porous surface with suction and injection, Discret Contin Dyn Syst - Ser S, 11, 583–594. DOI: 10.3934/dcdss.2018033

Eastman J.A., Choi S.U.S., Li S., Yu W., Thompson L.J., 2001, Anomalously increased effective thermal conductivities of ethylene glycol-based nanofluids containing copper nanoparticles, Appl Phys Lett, 78,718–720. DOI: 10.1063/1.1341218

Choi S.U.S., Eastman J.A., 1995, Enhancing thermal conductivity of fluids with nanoparticles, Proc 1995 ASME Int Mech Engi- Neering Congr Expo SanFrancisco, USA, ASME, FED231/MD66, 99–105.

Cortell R., 2007, Viscous flow and heat transfer over a nonlinearly stretching sheet, Appl Math Comput 184, 864–873. DOI: 10.1016/j.amc.2006.06.077

Hong H., Wright B., Wensel J., Jin S., Ye X.R., Roy W., 2007, Enhanced thermal conductivity by the magnetic field in heat transfer nanofluids containing carbon nanotube, Synth Met, 157, 437–440. DOI: 10.1016/j.synthmet.2007.05.009

Hussain Z., Hayat T., Alsaedi A., Ahmad B., 2018, Three-dimensional convective flow of CNTs nanofluids with heat generation/absorption effect: A numerical study, Comput Methods Appl Mech Eng, 329, 40–54. DOI: 10.1016/j.cma.2017.09.026

Kumar P., Tanmoy K., Kalidas C., 2018, Framing the Cattaneo – Christov heat flux Phenomena on CNT-based Maxwell Nanofluid along stretching sheet with multiple slips, Arab J Sci Eng 43, 1177–1188. DOI: 10.1007/s13369-017-2786-6

Li Y., Lv H., 2018, Numerical Simulation of Mass Transfer of Slug Flow in Microchannel, Chemical Engineering Transactions, 65, 325-330, DOI:10.3303/CET1865055

Miklavcic M., Wang C.Y., 2006, Viscous flow due to a shrinking sheet, Q Appl Math LXIV, 283–290. DOI: 10.1090/S0033-569X-06-01002-5

Pal D., Mandal G., Vajravelu K., 2013, MHD convection-dissipation heat transfer over a non-linear stretching and shrinking sheets in nanofluids with thermal radiation, Int J Heat Mass Transf 65, 481–490. DOI: 10.1016/j.ijheatmasstransfer.2013.06.017

Rashid I., Ul Haq R., Al-Mdallal Q.M., 2017, Aligned magnetic field effects on water based metallic nanoparticles over a stretching sheet with PST and thermal radiation effects, Phys E Low-Dimensional Syst Nanostructures, 89, 33–42. DOI: 10.1016/j.physe.2017.01.029

Reddy P.B.A., Reddy N.B., Palani G., 2012, Convective flow past a vertical plate under the influence of magnetic field and thermal radiation subjected to a variable surface temperature in the presence of heat source/sink, Thermophys Aeromechanics, 19, 489–501. DOI: 10.1134/S0869864312030146

Ul Haq R., Nadeem S., Khan Z.H., Noor N.F.M., 2015, Convective heat transfer in MHD slip flow over a stretching surface in the presence of carbon nanotubes, Phys B Condens Matter, 457, 40–47. DOI: 10.1016/j.physb.2014.09.031

Wang CY., 2008, Stagnation flow towards a shrinking sheet, Int J Non-Linear Mech, 43, 377–382. DOI: 10.1016/j.ijnonlinmec.2007.12.021

Xuan Y., Li Q., 2003, Investigation on convective heat transfer and flow features of nanofluids, J Heat Transfer, 125, 151–155. DOI: 10.1115/1.1532008